

# Impedance Spectroscopy of Tripolar Concentric Ring Electrodes with Ten20 and TD246 Pastes

Seyed Hadi Nasrollahhosseini, *Member, IEEE*, Daniel Salazar Herrera, *Member, IEEE*  
Walter G. Besio, *Senior Member, IEEE*

**Abstract**—Electrodes are used to transform ionic currents to electrical currents in biological systems. Modeling the electrode-electrolyte interface could help to optimize the performance of the electrode interface to achieve higher signal to noise ratios. There are previous reports of accurate models for single-element biomedical electrodes. In this paper, we measured the impedance on both tripolar concentric ring electrodes and standard cup electrodes by electrochemical impedance spectroscopy (EIS) using both Ten20 and TD246 electrode paste. Furthermore, we applied the model to prove that the model can predict the performance of the electrode-electrolyte interface for tripolar concentric ring electrodes (TCRE) that are used to record brain signals.

## I. INTRODUCTION

Physiological systems such as cardiovascular system, nervous system, and muscular system all generate ionic current flows in the body. Each physiological process is associated with specific signals that reflect the underlying nature and activities of each source. One such physiological signal of interest is the electroencephalography (EEG) which is the recording of brain electrical activity. Brain signals, like other biomedical signals, can be obtained with electrodes that sense the variations in electrical potential generated by physiological processes. Electrodes convert the ionic currents flowing in the body generated by underlying cells into electrical currents [1]. Therefore, we need to understand the mechanisms that generate the transduction process between the electrode and human body. Equivalent circuit models of the electrode, electrolyte, and body may help us to have a better understanding of how biomedical signals are obtained by electrodes.

At the contact site of an electrode to the body an electrode-electrolyte interface forms. The contact of an electrode to electrolyte is depicted in Fig. 1. At the interface of electrode-electrolyte, chemical reactions take place that can be shown by the following equations [2]:

Research supported by NSF award 1539068 to WB. The content is solely the responsibility of the authors and does not necessarily represent the official views of the National Science Foundation.

S. H. Nasrollahhosseini is with the Electrical, Computer, and Biomedical Engineering Department, University of Rhode Island, Kingston, RI 02881 USA, (e-mail: hadi@ele.uri.edu).

D. S. Herrera is with the Electrical, Computer, and Biomedical Engineering Department, University of Rhode Island, Kingston, RI 02881 USA, (email: dansal10@my.uri.edu)

W. G. Besio is with the Electrical, Computer, and Biomedical Engineering Department, University of Rhode Island, Kingston, RI 02881 USA, (e-mail: besio@uri.edu).

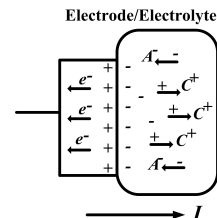
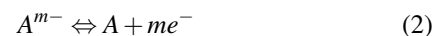


Fig. 1. Electrode-Electrolyte Interface



Obtaining an accurate model for the electrode-electrolyte interface is complicated and has been studied for many years. First, Helmholtz in 1879, proposed the concept of electric double layer [3]. He realized that at the electrode-electrolyte interface, since the electrolyte is saturated with charged electrons, the ions with the same charges will be pushed back while the opposite charges will be attracted. Therefore, at the electrode-electrolyte interface there will be two compact layers of opposite charges called the electric double layer (EDL). Warburg, in 1899, proposed a series combination of a capacitor and resistor in which the magnitude of the reactance and resistance is dependent on the electrode type, area (including surface conduction), electrolyte, frequency, and the current density [4]. In 1932 Fricke proposed a similar model for the electrode-electrolyte interface with the Warburg combination of series resistor and capacitor, adding that  $C_W = \frac{K}{\omega^m}$  (k and m depend on the metal species) which reveals the frequency dependants of the capacitance. In 1947 Randles suggested another popular model that include a double-layer capacitance in parallel with a series combination of resistance and capacitance. In 1968 [4], Geddes and Baker proposed another model that considers the passage of DC through the interface. In their model the Warburg capacitance is in parallel with the Faradic resistance to model the property of DC that passes through the interface. In [5], the author proposed a circuit model for the tripolar concentric ring electrode and compared the model with the conventional cup electrode. Their model is shown in Fig. 3 and is described in section II.

In this paper, we measured the impedance on both tripolar concentric ring electrodes and standard cup electrodes by

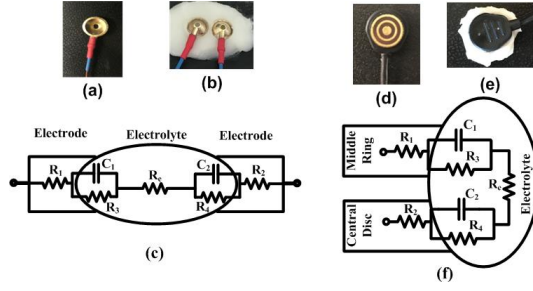


Fig. 2. Cup electrode (a), cup electrodes placed on Ten20 paste (b), electrical circuit model of the cup electrode placed on an electrolyte (c), TCRE electrode (d) TCRE placed on Ten20 paste (e), electrical circuit model of the TCRE placed on an electrolyte (f)

electrochemical impedance spectroscopy (EIS) using both Ten20 and TD246 electrode paste. Furthermore, we applied the model that is proposed in [5] to prove that the model can predict the performance of the electrode.

The rest of the paper is organized as follows. The equivalent circuit model for the tripolar concentric ring electrode is explained in section II. The procedure of the measurement is addressed in section III. Section IV presents the results concluded by section V.

## II. EQUIVALENT CIRCUIT MODEL

Electroencephalography (EEG) is one of the mainstays of hospital diagnostic procedures and pre-surgical planning. End users struggle with EEGs poor spatial resolution, selectivity and low signal-to-noise ratio, limiting its effectiveness in research discovery and diagnosis [6]-[7]. Tripolar concentric ring electrodes (TCREs), consisting of three elements including the outer ring (inner radius is 4.4mm and outer radius is 5mm), the middle ring (inner radius is 2.5mm and outer radius is 3.2mm), and the central disc (radius is 1.4mm) (Fig. 2d, e), are distinctively different from conventional cup electrodes that have a single element (Fig. 2a, b). TCREs have been shown to estimate the surface Laplacian directly [8]. The Laplacian algorithm is two-dimensional and weights the middle ring and central disc signal difference sixteen times greater than the outer ring and central disc signal difference [8]. Compared to EEG with conventional cup electrodes Laplacian EEG using TCREs (tEEG) have been shown to have significantly better spatial selectivity (approximately 2.5 times higher), signal-to-noise ratio (approximately 3.7 times higher), and mutual information (approximately 12 times lower) [9].

Fig. 2a illustrates a conventional cup electrode. Fig. 2b shows the cup electrodes placed in the fresh Ten20 (Weaver and Company) paste as a skin-to-electrode electrolyte, similar as in real recordings, to mimic the body. The equivalent circuit model for this configuration is shown in Fig. 2c. TCRE electrode is also depicted in Fig. 2d, and Fig. 2e shows the TCRE electrode is placed in fresh Ten20 paste. Therefore, there is an electrode-electrolyte interface between

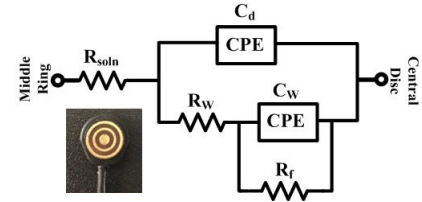


Fig. 3. Electrical model for the tri-polar concentric ring electrode

each pair of rings of the TCRE. Fig. 2f illustrates part of the electrical model representation for the TCRE electrode-electrolyte interface between the central disc and middle ring. In both models  $R_1$ ,  $C_1$  and  $R_2$ ,  $C_2$  are the equivalent series resistances and capacitances of the two electrode-electrolyte interfaces. The  $R_e$  represents the electrolyte resistance, and the resistances  $R_3$  and  $R_4$  are the equivalent resistances for the leakage current of the electrode-electrolyte interface. Therefore, if we neglect  $R_3$  and  $R_4$  for simplicity, the impedance that is seen between the middle ring to the central disc  $Z_{DM}$  is:

$$Z_{DM} = R_1 + \frac{1}{j\omega C_1} + R_e + \frac{1}{j\omega C_2} + R_2 \quad (3)$$

And the resistive part is:

$$R_{DM} = R_1 + R_e + R_2 \quad (4)$$

where  $R_e = \rho \frac{L}{A}$  is an ionic solution resistance that depends on the ionic concentration, types of the ions, temperature and the area in which current is carried, and  $\rho$  is the solution resistivity. And the reactive part is:

$$\frac{1}{C_{DM}} = \frac{1}{C_1} + \frac{1}{C_2} \quad (5)$$

Based on the above mentioned parameters, and with the aid of the non-linear least squares fitting program of the electrochemical impedance spectroscopy (EIS), the authors proposed in [5] a model for the TCREs that is depicted in Fig. 3. In this model,  $R_{soln}$  is the equivalent solution (electrolyte) resistance,  $C_d$  represents the equivalent double layer capacitance,  $R_W$  and  $C_W$  are the equivalent Warburg combination, and  $R_f$  represents the equivalent leakage current in the electrode-electrolyte interface. For a perfect match of the model with the experimental data, a constant phase element (CPE) was used instead of capacitors. This is due to the "double layer capacitors" often behaves like a CPE instead of a pure capacitor [10], [11]. The impedance of a double layer capacitor has the form:

$$Z_{CPE} = \frac{1}{Q(j\omega)^\alpha} \quad (6)$$

In (6), if the constant  $\alpha = 1$ , the equation describes capacitance and  $Q$  has units of capacitance. Otherwise, if  $0 < \alpha < 1$ , the equation represent the CPE and  $Q$  has units of  $Fcm^{-2}s^{(\alpha-1)}$ ,  $\frac{s^\alpha}{\Omega}$ .

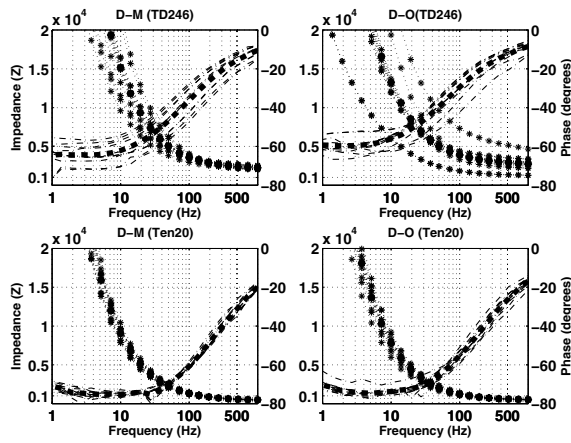


Fig. 4. Bode plots of TCRE, central disc to outer ring (D-O) and central disc to middle ring (D-M) with Ten20 and TD246 pastes (10 experiments with average of them that the averaged in each graph is shown in bold) (asterisks are the impedance and phases are shown with dashed lines).

### III. PROCEDURE

In order to measure impedances on both TCREs and standard cup electrodes, we performed electrochemical impedance spectroscopy (EIS) ten times each, using both Ten20 (Weaver Company) and TD-246 (Florida Research Instruments) electrode pastes. Both pastes are meant to serve as skin-to-electrode electrolytes, however the difference between the two is in their viscosity, and furthermore in their application. The Ten20 paste has a higher viscosity and therefore can be directly applied to the head with an electrode attached. Meanwhile, the TD-246 paste is much less viscous and requires the use of an electrode cap to assist in the adhesion of the electrode to the paste on the head. For our experiments we applied the paste on to a plastic plate and attached the electrodes directly to the paste in order to mimic the skin-to-electrode contact. To perform EIS measurements with both of these electrode pastes, we used the Gamry potentiostatic instrument framework. The system was configured in order to perform two-electrode measurements. This allowed us to measure the impedances between the middle ring and central disc (M-D) of the TCREs, as well as the impedances between the outer ring and central disc (O-D). We also measured the impedances between two standard cup electrodes as reference. When measuring the impedance between middle ring and central disc we connected the blue (working sense) and green (working current) leads to the middle ring and the white (reference) and red (counter current) leads to the central disc. The same setup was used while measuring impedance between the outer ring and central disc, the only difference is the blue and green leads were now connected to the outer ring. The two standard cup electrodes were also connected in the same manner, with no specification as to which one went to green and blue leads or white and red leads. These were placed as close together on the same span of paste in order to resemble the measurements with the TCRE.

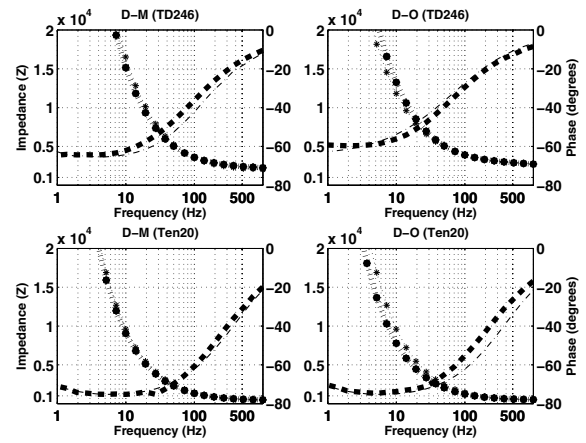


Fig. 5. The averaged impedance and phase with the fit curves with the model for TCRE, central disc to outer ring (D-O) and central disc to middle ring (D-M) with Ten20 and TD246 pastes (averaged in each graph is shown in bold) (asterisks are the impedance and phases are shown with dashed lines).

### IV. RESULTS

The Bode plots for the TCRE between the central disc to middle ring (D-M) and the central disc to outer ring (D-O) using both Ten20 and TD246 paste are shown in Fig. 4. In each setup 10 experiments were run in order to reduce nuisance variables such as environmental noise. The bold line in the Bode plots represents the average of the ten experiments. The linear curve fits from the model, of impedances for the TCRE (D-M) rings and TCRE (D-O) rings are shown in Fig. 5, as well as the averaged curves. The model that is shown in Fig. 3 is used for the linear fit curves. As Fig. 5 shows, the fit curve matches the averaged curve. Therefore, the model in Fig. 3 can predict the performance of the TCRE.

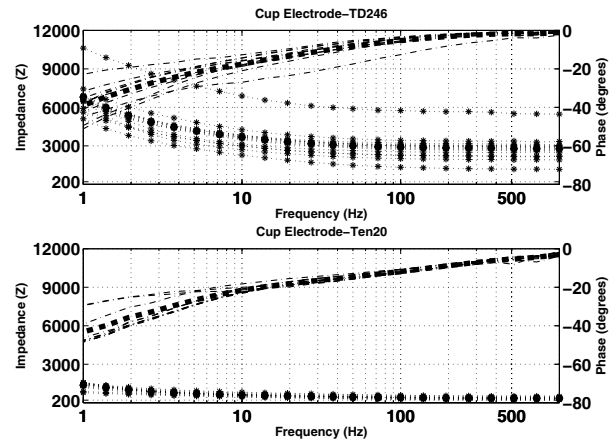


Fig. 6. Bode plots of conventional cup electrode with Ten20 and TD246 pastes (10 experiments with average of them that the averaged in each graph is shown in bold) (asterisks are the impedance and phases are shown with dashed lines).

TABLE I  
PARAMETER VALUES FOR THE TEEG MODEL

Parameters	TCRE (DM) 1020 Paste	TCRE (DO) 1020 Paste	TCRE (DM) TD-246 Paste	TCRE (DO) TD-246 Paste	Standard Disc 1020 Paste	Standard Disc TD-246 Paste
<b>R<sub>soln</sub></b> (ohms)	397.4 ± 3.501	435.3 ± 3.897	2.37e+03 ± 23.62	2.63e+03 ± 23.61	353.4 ± 3.291	2.15e+03 ± 16.38
<b>R<sub>cor</sub></b> (ohms)	2.03e+05 ± 4.94e+04	4.17e+05 ± 1.55e+05	1.82e+07 ± 1.62e+09	1.89e+04 ± 2.67e+13	1.829 ± 1.22e+08	5.20e+05 ± 1.02e+05
<b>R<sub>po</sub></b> (ohms)	5.40e+05 ± 3.14e+04	3.15e+05 ± 1.24e+05	9.86e+05 ± 9.47e+05	5.52e+06 ± 5.96e+12	3.71e+05 ± 1.21e+08	4.24e+03 ± 1.98e+03
<b>C<sub>cor</sub></b> ( $\frac{s}{\Omega}$ )	2.16e-05 ± 1.09e-05	2.93e-06 ± 2.05e-06	3.73e-06 ± 8.19e-06	1.00e-04 ± 6.52e+04	1.11e-01 ± 1.14e+07	2.21e-05 ± 8.39e-06
<b>n</b>	1.00 ± 1.66	6.26e-01 ± 1.58e-01	2.55e-01 ± 1.03	6.36e-03 ± 7.65e+06	5.44e-01 ± 1.76e+06	8.63e-01 ± 8.50e-02
<b>C<sub>c</sub></b> ( $\frac{s}{\Omega}$ )	2.87e-06 ± 4.89e-08	3.06e-06 ± 1.06e-07	1.10e-06 ± 4.47e-08	4.67e-06 ± 4.17e-07	2.11e-04 ± 8.22e-05	3.32e-05 ± 7.90e-06
<b>m</b>	8.70e-01 ± 3.41e-03	8.68e-01 ± 5.91e-03	7.53e-01 ± 6.49e-03	7.29e-01 ± 1.43e-02	6.67e-01 ± 6.28e-02	7.36e-01 ± 3.64e-02

Fig. 6 shows the standard cup electrode Bode plots using both Ten20 and TD-246 paste. Observing Fig. 4, 5 and 6 there are two items to notice: (1) the TCRE phase only varies from 70 to 60 degrees with the Ten20 paste and 40 to 60 with TD246 paste in the frequency band 1Hz to 100Hz while the cup electrode phase varies from 50 to 10 degrees with both Ten20 and TD-246; and (2) the impedance of the TCRE is below 5k $\Omega$  from 10Hz and beyond with the Ten20 and is below 10k $\Omega$  with TD246 whereas the cup electrode impedance is below 6k $\Omega$  beyond 1Hz for TD-246 and is below 1k $\Omega$  beyond 1Hz for the Ten20.

Table 1 shows the parameter values of the equivalent circuit model that is depicted in Fig. 3 for the TCRE (D-O) rings, TCRE (D-M) rings, and standard cup electrodes using both Ten20 and TD246 paste. With the Ten20 paste the parameter values  $R_{soln}$ ,  $R_{po}$ ,  $n$ , and  $m$  were similar in all models (TCRE, (D-M), TCRE (D-O), and standard cup electrodes). However, the  $R_{soln}$ ,  $C_{cor}$ , and  $C_c$  parameter values were higher in the TCRE models than the standard cup electrode models. With the TD246 paste the  $R_{soln}$ ,  $R_{po}$ ,  $n$ , and  $m$  parameter values were similar across all models. The  $R_{cor}$  value for the TCRE (D-O) model was similar to the standard cup electrode, but the value for the TCRE (D-M) model was higher than that of the standard cup electrode. Lastly the  $R_{po}$  parameter value was higher among both TCRE models than the standard cup electrode model.

## V. CONCLUSION

In conclusion, we find that our model can predict the components for different materials used for impedance matching. We also found that the impedances for the TD246 between the electrodes was higher than those for Ten20 paste. Furthermore, we found that the phase between two conventional disc electrodes varied more with frequency than the phase for the TCREs.

## ACKNOWLEDGMENT

The authors would like to thank would like to thank Dr. Richard Brown for allowing us to use the Gamry potentiostatic instrument framework machine.

## REFERENCES

- [1] L. A. Geddes and L. E. Baker, *Principles of applied biomedical instrumentation*, (Wiley-Interscience, New York, 1975).
- [2] C. Boccaletti, F. Castrica, G. Fabbri, and M. Santello, *A non-invasive biopotential electrode for the correct detection of bioelectrical currents*, In Proceedings of the Sixth IASTED International Conference on Biomedical Engineering, pp. 353-358. ACTA Press, 2008.
- [3] Wang, Hainan and L. Pilon, *Accurate simulations of electric double layer capacitance of ultra microelectrodes*, The Journal of Physical Chemistry C115, no. 33 (2011): 16711-16719.
- [4] L. A. Geddes, *Historical evolution of circuit models for the electrode-electrolyte interface*, Annals of Biomedical Engineering, Vol. 25, pp. 1-14, 1997.
- [5] S. H. Nasrollahhosseini, P. Steele and W. G. Besio, *Electrode-electrolyte interface model of tripolar concentric ring electrode and electrode paste*, In Engineering in Medicine and Biology Society (EMBC), 2016 IEEE 38th Annual International Conference of the, pp. 2071-2074. IEEE, 2016.
- [6] J. E. Desmedt, V. Chalklinand, and C. Tomberg, *Emulation of somatosensory evoked potential (SEP) components with the 3-shell head model and the problem of 'ghost potential fields' when using an average reference in brain mapping.*, Electroenceph. Clin. Neurophysiol., vol. 77, pp. 243-258, 1990.
- [7] P. L. Nunez, R. B. Silberstein, P. J. Cadiush, J. Wijesinghe, A. F. Westdorp, and R. Srinivasan, *A theoretical and experimental study of high resolution EEG based on surface laplacians and cortical imaging*, EG and Clin. Neurophysiology, vol. 90, pp. 40-57, 1994.
- [8] W. G. Besio, K. Koka, W. Aakula, and W. Dai, *Tri-polar concentric ring electrode development for Laplacian electroencephalography*, IEEE Trans Biomed Eng, vol. 53, pp. 926-933, 2006.
- [9] K. Koka and W. G. Besio, *Improvement of spatial selectivity and decrease of mutual information of tri-polar concentric ring electrodes*, Journal of neuroscience methods, vol. 165, pp. 216-222, 2007.
- [10] B. Hirschorn, M. E. Orazem, B. Tribollet, V. Vivier, I. Frateur, and M. Musiani, *Constant-phase-element behavior caused by resistivity distributions in films I. Theory*, Journal of The Electrochemical Society 157, no. 12 (2010): C452-C457.
- [11] J. H. Chang, J. Park, Y. K. Pak, and J. J. Pak, *Fitting improvement using a new electrical circuit model for the electrode-electrolyte interface*, In Neural Engineering, 2007. CNE'07. 3rd International IEEE/EMBS Conference on, pp. 572-574. IEEE, 2007.